

Fluctuations and correlations in Kerr optical frequency combs with additive Gaussian noise

Cite as: Chaos **30**, 083146 (2020); <https://doi.org/10.1063/5.0006303>

Submitted: 03 March 2020 . Accepted: 11 August 2020 . Published Online: 31 August 2020

Yanne K. Chembo , Aurélien Coillet , Guoping Lin, Pere Colet , and Damià Gomila 



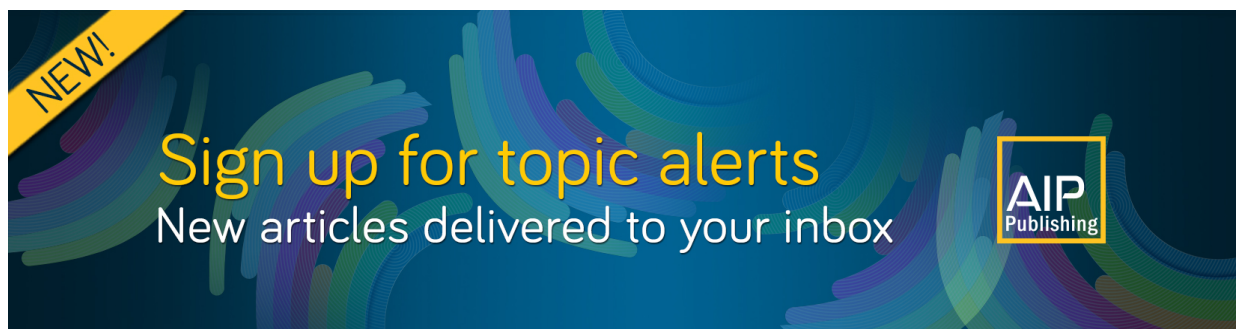
View Online



Export Citation



CrossMark



NEW!

Sign up for topic alerts
New articles delivered to your inbox

AIP
Publishing



Fluctuations and correlations in Kerr optical frequency combs with additive Gaussian noise

Cite as: Chaos 30, 083146 (2020); doi: 10.1063/5.0006303

Submitted: 3 March 2020 · Accepted: 11 August 2020 ·

Published Online: 31 August 2020



View Online



Export Citation



CrossMark

Yanne K. Chembo,^{1,a)} Aurélien Coillet,² Guoping Lin,³ Pere Colet,⁴ and Damià Gomila⁴

AFFILIATIONS

¹Department of Electrical and Computer Engineering, University of Maryland and Institute for Research in Electronics and Applied Physics (IREAP), 8279 Paint Branch Dr., College Park, Maryland 20742, USA

²Laboratoire Interdisciplinaire Carnot de Bourgogne, CNRS and Univ. Bourgogne-Franche-Comté, 9 Avenue A. Savary, 21078 Dijon, France

³Key Lab of Micro-Nano Optoelectronic Information System, Ministry of Industry and Information Technology, School of Science, Harbin Institute of Technology, Shenzhen 518055, China

⁴Instituto de Física Interdisciplinar y Sistemas Complejos, IFISC (CSIC-UIB), Campus Universitat de les Illes Balears, E-07122 Palma de Mallorca, Spain

Note: This article is part of the Focus Issue, instabilities and Nonequilibrium Structures.

^{a)}Author to whom correspondence should be addressed: ykchembo@umd.edu

ABSTRACT

We investigate the effects of environmental stochastic fluctuations on Kerr optical frequency combs. This spatially extended dynamical system can be accurately studied using the Lugiato–Lefever equation, and we show that when additive noise is accounted for, the correlations of the modal field fluctuations can be determined theoretically. We propose a general theory for the computation of these field fluctuations and correlations, which is successfully compared to numerical simulations.

Published under license by AIP Publishing. <https://doi.org/10.1063/5.0006303>

Nonlinear phenomena in ultrahigh Q whispering-gallery mode (WGM) resonators have attracted a great deal of interest in recent years. Typically, a resonance is pumped by a continuous-wave laser, and neighboring sidemodes are excited via the bulk nonlinearity of the resonator. Due to the possibility of chip-scale integration and power-efficient operation, they have provided an important and alternate way to produce frequency combs for both fundamental research and practical applications. Many of these applications require the combs to operate in an ultra-low-noise regime, where they feature the highest temporal coherence. The understanding of the interaction of external noise with the nonlinear dynamics of the intracavity field would permit the design of optimal strategies to ensure the highest performance for technological applications.

I. INTRODUCTION

In the last decade, nonlinear phenomena in ultrahigh-Q whispering-gallery mode (WGM) resonators emerged as one of the

major research topics in photonics.^{1–5} This exceptional amount of interest has been driven by the promise of important technological breakthroughs for several applications such as optical filtering, modulation, and multimode lasing, just to name a few.

When the intracavity bulk medium is amorphous or centrosymmetric, the prevalent nonlinear interaction is the Kerr effect. As a resonator is pumped by a continuous-wave (CW) laser, the small volume of confinement, high photon density, and long photon lifetime induce a very strong light–matter interaction, which may excite the neighboring eigenmodes via four-wave mixing.^{6,7} These cascaded photonic interactions ultimately yield a dissipative pattern in the spatial domain (resonator cavity) and an optical frequency comb—or the Kerr comb—in the spectral domain.⁸

The deterministic dynamics of Kerr combs is quite well understood today, and a comprehensive overview of this topic has been offered in Ref. 9. However, the effect of noise on these combs has been largely disregarded at this date, despite their critical importance. Indeed, any external noise excitation is mixed and redistributed in the comb in a nontrivial fashion that requires a dedicated study. A deep understanding of this noise mixing process

is critical for almost all the applications related to Kerr combs, as noise in this context directly translates to shorter temporal coherence, a higher signal-to-noise ratio, and ultimately decreased performance in applications such as coherent optical communications¹⁰ or microwave generation.¹¹

The objective of this work is, therefore, to provide a general framework to analyze the effect of additive noise in Kerr combs. We aim at showing that once the power of this noise is known, it is possible to calculate the amplitude of the stochastic fluctuations for each mode, as well as the cross correlations among them.

The article is organized as follows. Section II presents the model for the stochastic Kerr comb analysis, while Sec. III is devoted to the calculation of the fluctuation correlations. A specific case of interest is the one of primary combs originating from roll (Turing) patterns, for which we perform numerical simulations to test the validity of our analytical predictions in Sec. IV. Section V concludes the article.

II. THE STOCHASTIC MODEL

The deterministic dynamics of Kerr combs can be accurately investigated using the Lugiato–Lefever equation (or LLE—see Refs. 12 and 13 for a wider perspective). This equation governs the spatiotemporal evolution of the intracavity laser field in the whispering-gallery mode resonator.^{14–16} Depending on the frequency and power of the pump laser, various dynamical states can be excited, such as roll patterns, bright and dark solitons, breathers, and hyperchaos. An understanding on the stability properties of these patterns can be achieved via the spatial stability analysis of the flat solutions^{17,18} or using other techniques such as the normal form theory.^{19–22}

The LLE with additive external noise can be written as

$$\frac{\partial \psi}{\partial \tau} = -(1 + i\alpha)\psi + i|\psi|^2\psi - i\frac{\beta}{2}\frac{\partial^2 \psi}{\partial \theta^2} + F + \zeta(\theta, \tau), \quad (1)$$

where $\psi(\theta, \tau)$ is the complex amplitude of the overall field in the cavity, $\theta \in [-\pi, \pi]$ is the azimuthal angle along the cavity circumference, $\tau = t/2\tau_{\text{ph}}$ is the normalized time, with $\tau_{\text{ph}} = 1/2\kappa$ being the photon lifetime, $2\kappa = \omega_0/Q_{\text{tot}}$ the loaded linewidth, and Q_{tot} the loaded quality factor. The parameter $\alpha = -(\omega_L - \omega_0)/\kappa$ stands for the detuning between the pump laser and the cold resonance frequencies ω_L and ω_0 , respectively. The parameter β represents the second-order dispersion of the resonator, while F stands for the amplitude of the pump laser field. The external complex-valued noise perturbation is considered white and Gaussian with the correlation

$$\langle \zeta(\theta, \tau)\zeta^*(\theta', \tau') \rangle = \Gamma\delta(\theta - \theta')\delta(\tau - \tau') \quad (2)$$

and the mean value $\langle \zeta(\theta, \tau) \rangle = 0$, where Γ is the noise square amplitude and $\delta(x)$ the usual Kronecker function equal to 1 for $x = 0$ and to 0 otherwise. The Gaussian noise can be interpreted at the most fundamental level as the vacuum fluctuations entering the cavity, and its amplitude can be derived from a quantum model.³⁶ However, in practice, this noise will result in first approximation from all the environmental fluctuations influencing the experimental system. Throughout this article, we consider $\Gamma = 1.6 \times 10^{-7}$.

The intracavity field can be decomposed according to the following modal expansion:

$$\psi(\theta, \tau) = \sum_l \psi_l(\tau)e^{il\theta}, \quad (3)$$

with $l = \ell - \ell_0$ being the azimuthal eigennumber of the photons with respect to the pumped mode (the pumped mode is, therefore, $l = 0$, while the sidemodes correspond to $l = \pm 1, \pm 2, \dots$). In this analysis, we will consider a comb spanning from $l = -N$ to $l = N$, that is, a comb that can potentially have $2N + 1$ modes overall.

By plugging the expansion of Eq. (3) inside the LLE, the following set of ordinary differential equations ruling the dynamics of each mode is obtained:

$$\begin{aligned} \dot{\psi}_l = & \left[-(1 + i\alpha) + i\frac{\beta}{2}l^2 \right] \psi_l + \delta(l)F \\ & + i \sum_{m,n,p} \delta(m - n + p - l) \psi_m \psi_n^* \psi_p + \zeta_l(\tau), \end{aligned} \quad (4)$$

where the overdot denotes the derivative relatively to the dimensionless time τ , while m, n, p , and l are eigennumbers labeling the interacting modes following the interaction $\hbar\omega_m + \hbar\omega_p \leftrightarrow \hbar\omega_n + \hbar\omega_l$. The modal noise excitation terms are obtained by Hermitian projection as

$$\zeta_l(\tau) = \frac{1}{2\pi} \int_{-\pi}^{\pi} \zeta(\theta, \tau) e^{-il\theta} d\theta, \quad (5)$$

which actually correspond to the Fourier spectral density of the noise at the frequency corresponding to the mode l . The corresponding correlation is, therefore,

$$\langle \zeta_l(\tau)\zeta_l^*(\tau') \rangle = \Gamma\delta(l - l')\delta(\tau - \tau') \quad (6)$$

and is also Gaussian and white.

Figure 1 proposes a schematic representation of noisy dissipative patterns and their corresponding combs. Our objective will be to evaluate the amplitude of the stochastic fluctuations for each mode, as well as the correlations among them.

III. FLUCTUATION CORRELATIONS IN STOCHASTIC KERR COMBS

In order to compute the correlations between the modal fluctuations, we consider a stationary Kerr comb spanning from $l = -N$ to $l = N$ (a total of $2N + 1$ modes). The steady state amplitude of the oscillating modes obey the set of $(2N + 1)$ nonlinear algebraic equations with $l = -N, \dots, N$,

$$\begin{aligned} & \left[-(1 + i\alpha) + i\frac{\beta}{2}l^2 \right] \psi_l + \delta(l)F \\ & + i \sum_{m,n,p} \delta(m - n + p - l) \psi_m \psi_n^* \psi_p = 0. \end{aligned} \quad (7)$$

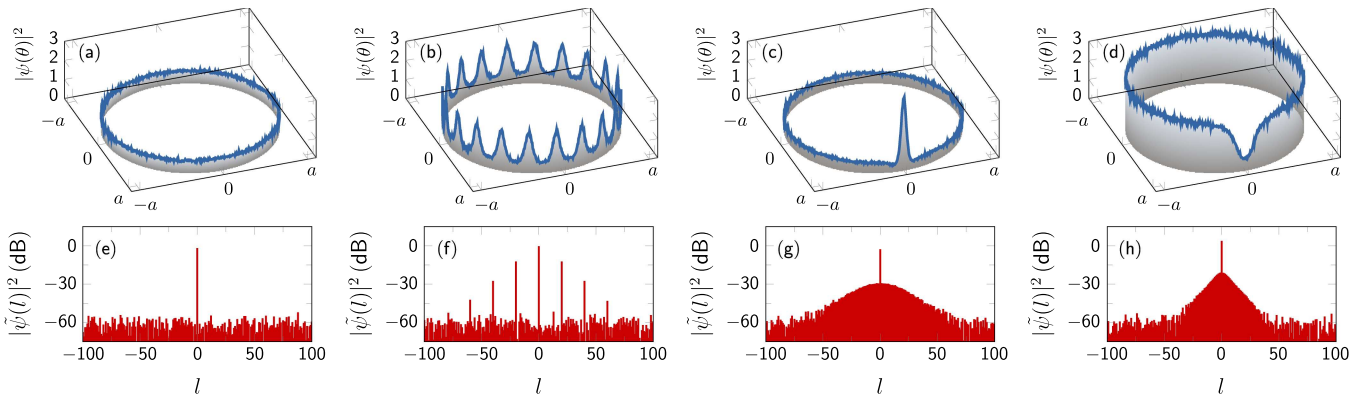


FIG. 1. Schematic representation in space [(a)–(d)] and frequency [(e)–(h)] of a stochastic Kerr comb at a given time t (snapshot). The upper row displays the intra-cavity field intensity $|\psi|^2$, while the lower row displays the corresponding stem plot for the modal intensities $|\psi_l|^2 \equiv |\tilde{\psi}(l)|^2$ in a logarithmic scale (note that these are technically not Fourier spectra, for being snapshots). The study of these stochastic fluctuations can be extended to those of quantum fluctuations (see Ref. 23). (a) and (e) Flat state. (b) and (f) Roll (Turing) pattern of order $L = 20$. (c) and (g) Bright soliton. (d) and (h) Dark soliton.

The noise driven fluctuations are ruled by the following set of equations, obtained after linearizing Eq. (4) around the solution (7):

$$\begin{aligned} \delta\dot{\psi}_l = & \left[-(1 + i\alpha) + i\frac{\beta}{2}l^2 \right] \delta\psi_l \\ & + i \sum_{m,n,p} \delta(m - n + p - l) \{ \delta\psi_m \psi_n^* \psi_p \\ & + \psi_m \delta\psi_n^* \psi_p + \psi_m \psi_n^* \delta\psi_p \} + \zeta_l(\tau). \end{aligned} \quad (8)$$

The above equation can be synthetically rewritten as

$$\delta\dot{\psi}_l = \sum_{p=-N}^N \mathbf{R}_{lp} \delta\psi_p + \sum_{p=-N}^N \mathbf{S}_{lp} \delta\psi_p^* + \zeta_l(\tau), \quad (9)$$

where

$$\begin{aligned} \mathbf{R}_{lp} = & \left[-(1 + i\alpha) + i\frac{\beta}{2}l^2 \right] \delta(p - l) \\ & + 2i \sum_{m,n} \delta(m - n + p - l) \psi_m \psi_n^*, \end{aligned} \quad (10)$$

$$\mathbf{S}_{lp} = i \sum_{m,n} \delta(m + n - p - l) \psi_m \psi_n \quad (11)$$

can be considered as the elements of the $(2N + 1)$ th-order square matrices \mathbf{R} and \mathbf{S} .

If we introduce the $(2N + 1)$ -dimensional fluctuation and noise vectors

$$\delta\mathbf{\Psi}(\tau) = \begin{bmatrix} \delta\psi_{-N}(\tau) \\ \vdots \\ \delta\psi_N(\tau) \end{bmatrix}, \quad \mathbf{Z}(\tau) = \begin{bmatrix} \zeta_{-N}(\tau) \\ \vdots \\ \zeta_N(\tau) \end{bmatrix}, \quad (12)$$

then we can write Eq. (8) under the form of a noise-driven linear flow,

$$\begin{bmatrix} \delta\dot{\mathbf{\Psi}} \\ \delta\dot{\mathbf{\Psi}}^* \end{bmatrix} = \mathbf{J} \begin{bmatrix} \delta\mathbf{\Psi} \\ \delta\mathbf{\Psi}^* \end{bmatrix} + \begin{bmatrix} \mathbf{Z}(\tau) \\ \mathbf{Z}^*(\tau) \end{bmatrix}, \quad (13)$$

where

$$\mathbf{J} = \begin{bmatrix} \mathbf{R} & \mathbf{S} \\ \mathbf{S}^* & \mathbf{R}^* \end{bmatrix} \quad (14)$$

is a composite (block matrix) Jacobian of order $2(2N + 1)$. It is interesting to note that in Ref. 24, the flow of Eq. (13) is written by associating $\Re[\delta\mathbf{\Psi}]$ and $\Im[\delta\mathbf{\Psi}]$ instead of $\delta\mathbf{\Psi}$ and $\delta\mathbf{\Psi}^*$ as we have done here. This latter choice is motivated by the possibility to express the Jacobian matrix of the perturbation flow in a simple and explicit way. It should be noted that this Jacobian matrix has to be determined numerically (since its components exclusively depend on the steady state values of the various ψ_l).

If we consider that there is a matrix \mathbf{P} that diagonalizes \mathbf{J} to \mathbf{D} following $\mathbf{D} = \mathbf{P}\mathbf{J}\mathbf{P}^{-1}$, then we can introduce the $2(2N + 1)$ -dimensional diagonal field fluctuations and noise vectors as

$$\delta\mathbf{\Phi}(\tau) = \mathbf{P} \begin{bmatrix} \delta\mathbf{\Psi}(\tau) \\ \delta\mathbf{\Psi}^*(\tau) \end{bmatrix} \quad \text{and} \quad \mathbf{\Upsilon}(\tau) = \mathbf{P} \begin{bmatrix} \mathbf{Z}(\tau) \\ \mathbf{Z}^*(\tau) \end{bmatrix} \quad (15)$$

so that the stochastic flow is now diagonalized as

$$\delta\dot{\mathbf{\Phi}} = \mathbf{D} \delta\mathbf{\Phi} + \mathbf{\Upsilon}(\tau). \quad (16)$$

Note that $\delta\mathbf{\Phi}$ and $\mathbf{\Upsilon}$ have a dimension that is the double of the one of $\delta\mathbf{\Psi}$ and \mathbf{Z} , respectively. In particular, the noise vector in the diagonal base can be explicitly expanded as a linear combination of ζ_l and ζ_l^* following

$$\begin{aligned} \Upsilon_m = & \sum_{n=1}^{2N+1} \mathbf{P}_{mn} \zeta_{n-N-1} + \sum_{n=2N+2}^{4N+2} \mathbf{P}_{mn} \zeta_{n-3N-2}^* \\ = & \sum_{l=-N}^N \{ \mathbf{P}_{m,l+N+1} \zeta_l + \mathbf{P}_{m,l+3N+2} \zeta_l^* \}. \end{aligned} \quad (17)$$

It can straightforwardly be inferred that $\langle \Upsilon_m(\tau) \rangle = 0$, while the various correlations between the components of this noise vector are

$$\begin{aligned} \langle \Upsilon_m(\tau) \Upsilon_n^*(\tau') \rangle &= \Gamma_{mn} \delta(\tau - \tau'), \\ \langle \Upsilon_m(\tau) \Upsilon_n(\tau') \rangle &= \tilde{\Gamma}_{mn} \delta(\tau - \tau'), \end{aligned} \tag{18}$$

with

$$\begin{aligned} \Gamma_{mn} &= \Gamma \sum_{k=1}^{4N+2} \mathbf{P}_{km} \mathbf{P}_{kn}^*, \\ \tilde{\Gamma}_{mn} &= \Gamma \sum_{k=1}^{4N+2} \mathbf{P}_{km} \mathbf{P}_{kn}. \end{aligned} \tag{19}$$

The above equations permit the computation of the stochastic field amplitudes and cross correlations for any kind stationary comb, namely, roll patterns (sub- or supercritical) and solitons (bright, dark, or flaticons). It is worth emphasizing that the present work does not investigate the influence of noise on a bifurcation; it is about the effect on noise on a given pattern after the bifurcation has occurred. The underlying idea developed in this section is, therefore, not to linearize the pattern close to a bifurcation point, and then using that pattern profile further away, in which case, the effect of weakly nonlinear terms should be accounted for (see, for example, Ref. 25). Instead, here, we start from the fully nonlinear pattern for the parameters far away from the bifurcation point. Without noise, this pattern has a neutrally stable Goldstone mode associated with translational symmetry and otherwise is stable (all other perturbations are damped). In this work, we only linearize the effect of the noise on the pattern, which is reflected in the excitation of the Goldstone mode and the less damped modes (soft modes). We hereafter focus on the case of primary combs as they feature a particular structure where only a reduced set of modes is excited, while other modes are not.

IV. THE SPECIFIC CASE OF PRIMARY COMBS

Primary combs are the spectral signature of Turing (roll) patterns. In the spatial domain, Turing patterns feature an integer number L of rolls in the azimuthal direction, while in the frequency domain, they are characterized by combs with teeth separated by L times the free-spectral range, i.e., $l = 0, \pm L, \pm 2L, \dots$. Hence, in the case of a Turing pattern with the wavenumber L , Eq. (3) can be written as

$$\psi(\theta, \tau) = \sum_n \psi_n(\tau) e^{inL\theta}, \tag{20}$$

where $n = 0, \pm 1, \dots, \pm M$, and M is the integer part of N/L . Figure 2 shows an example of such solution for $\alpha = 1.5$ and $F = 1.2525$. Such patterns are found spontaneously above threshold starting from a random initial condition. Simulations of Eq. (1) including noise are done using a pseudospectral method where the linear terms in the Fourier space are integrated exactly, while the nonlinear ones are integrated using a first-order in time approximation.²⁴ Deterministic stationary solutions are found by solving Eq. (4) with a Newton method.

In this case, the Jacobian of Eq. (14) becomes block diagonal, with $L/2 + 1$ boxes. It results that the eigenvectors of each box take the form of Bloch waves,

$$\delta\psi_q(\theta, \tau) = \sum_n \delta\psi_{n,q}(\tau) e^{i(nL+q)\theta} + \sum_n \delta\psi_{n,-q}(\tau) e^{i(nL-q)\theta}, \tag{21}$$

where q is an integer number between $0 \leq q < L/2$ (the first Brillouin zone of the pattern) and which labels the corresponding box of the Jacobian. There are, therefore, $4M + 2$ eigenvalues $\lambda_{n,q}$ for each value of $q \neq 0$ and $2M + 1$ eigenvalues for $q = 0$. They can be ranked according to the real parts of their eigenvalues following $\Re[\lambda_{0,q}] \geq \Re[\lambda_{1,q}] \geq \dots \geq \Re[\lambda_{4M+2,q}]$. In Fig. 3, we plot the spectrum (left) and the real part of the eigenvalues as a function of q (right) where one can clearly distinguish the different branches of

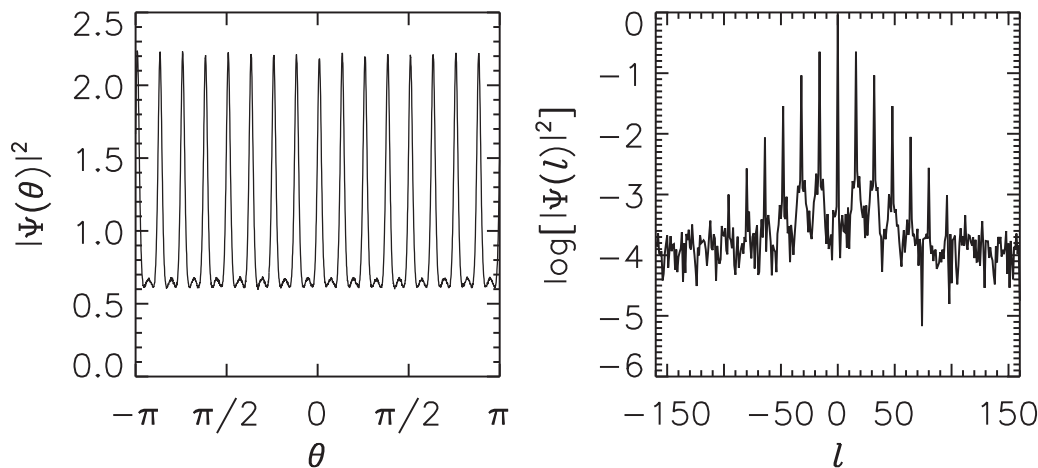


FIG. 2. Snapshot of a periodic pattern with the wavenumber ($L = 16$) in the ring cavity. The left panel shows the real field, while the right panel shows the Fourier transform of the pattern solution showing the corresponding frequency comb.

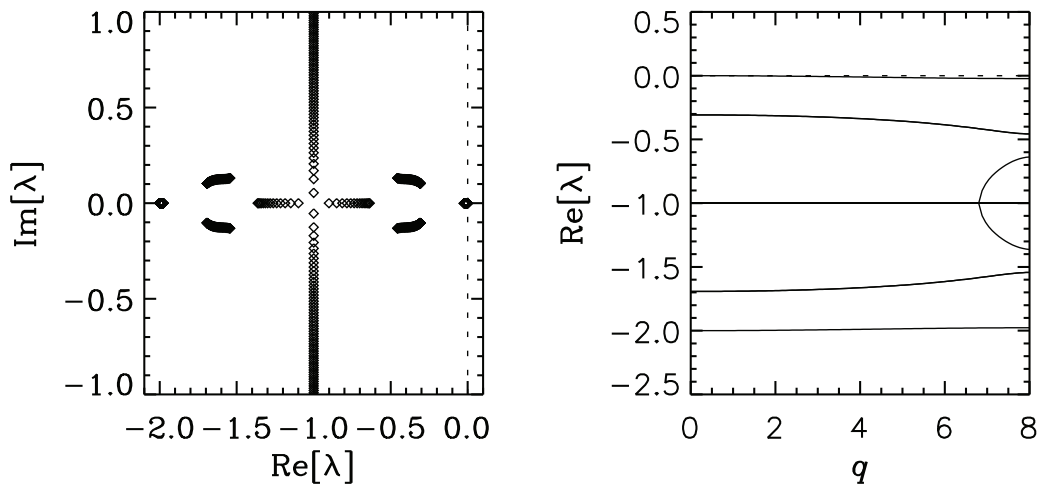


FIG. 3. Eigenvalues of the Turing pattern shown in Fig. 2. The full spectrum is shown on the left panel. On the right, we plot the real part of the eigenvalues as a function of the wavenumber q of the Bloch modes. Only the branches closer to zero are shown.

eigenvalues. The spectrum of the LLE shows a characteristic symmetry about the plain $\Re[\lambda] = -1$. We note also that there is a branch starting from $\Re[\lambda] = 0$. The mode with $\Re[\lambda] = 0$ at $q = 0$ is the Goldstone mode associated with the breaking of the translational invariance. The excitation of this mode changes only a global phase of the comb corresponding to the origin of the pattern in the real space. The modes of this branch with $q \sim 0$ are known as soft modes and describe long wavelength modulations of the phase of the pattern, what is known as phase dynamics.²⁸

Under the influence of noise, the dynamics of the amplitudes of the diagonal modes $\Phi_{n,q}$ follow,

$$\delta \dot{\Phi}_{n,q} = \lambda_{n,q} \Phi_{n,q} + \Upsilon_{n,q}(\tau), \tag{22}$$

which is, therefore, the reduced counterpart of Eq. (16) for roll patterns. The above equation is an Ornstein–Uhlenbeck process for the modes for which $\Re[\lambda_{n,q}] < 0$ and a Wiener process (or the Brownian motion) for the Goldstone mode with $\Re[\lambda_{0,0}] = 0$ (see Ref. 29). The formal solution corresponding to these stochastic processes is

$$\Phi_{n,q}(\tau) = \int_0^\tau e^{\lambda_{n,q}(\tau-s)} \Upsilon_{n,q}(s) ds \tag{23}$$

when the initial conditions are set to zero.

The correlations can be analytically calculated as in Ref. 24, and they asymptotically yield

$$\begin{aligned} \langle \Phi_{m,q}(\tau) \delta \Phi_{n,q}^*(\tau') \rangle &= \frac{\Gamma_{mn}^{(q)}}{-2(\lambda_{m,q} + \lambda_{n,q}^*)} \delta(\tau - \tau'), \\ \langle \Phi_{m,q}(\tau) \Phi_{n,q}(\tau') \rangle &= \frac{\tilde{\Gamma}_{mn}^{(q)}}{-2(\lambda_{m,q} + \lambda_{n,q})} \delta(\tau - \tau'), \end{aligned} \tag{24}$$

where the superscript (q) indicates that from (19), we take only the elements of the box corresponding to this wavenumber of the Bloch mode. In particular, the autocorrelation (mean square amplitude) of

the damped modes characterized by $\Re(\lambda_{n,q}) < 0$ can be calculated as

$$\langle |\Phi_{n,q}(\tau)|^2 \rangle = \frac{\Gamma_{nn}^{(q)}}{-4\Re(\lambda_{n,q})}, \tag{25}$$

while the Goldstone mode with $\Re(\lambda_{0,0}) = 0$ diffuses as

$$\langle |\Phi_{0,0}(\tau)|^2 \rangle = \frac{\Gamma_{00}^{(0)}}{4} \tau. \tag{26}$$

The divergence induced by the Goldstone mode does not invalidate the linear approximation, as the Goldstone mode is neutral at all orders and, therefore, it drifts indefinitely. The fluctuations of this neutral mode, however, do not hinder practical applications as it induces a change in the global phase of the frequency comb only. A change in this global phase corresponds to a shift of the pattern inside the cavity. The Goldstone mode does not change the intensity of the peaks.

The next modes contributing the most to the field fluctuations are the soft modes ($n = 0, q \gtrsim 0$). These modes correspond to long wavelength modulations of the phase, which in the frequency space correspond to exciting the modes nearby the main peaks, thus broadening them and ultimately limiting the precision of the frequency combs for measurements. Figure 4 shows the average square amplitude of the frequency comb fluctuations obtained both by direct numerical simulations with noise and analytically adding up the contributions of all modes given by Eq. (25). We first note that, according to (12) and (21), $\delta\psi_l = \psi_{n,q}$ such that $nL + q = l$. Then,

$$\langle |\delta\psi_{n,q}|^2 \rangle = \sum_l \sum_m P_{ln,q}^{-1} P_{mn,q}^{-1*} \langle \delta\Phi_{l,q} \delta\Phi_{m,q}^* \rangle, \tag{27}$$

where P_q^{-1} is the matrix that diagonalizes the block q of the Jacobian. There is a very good agreement between the linear analytical calculation and the numerical simulations of the full model. Two

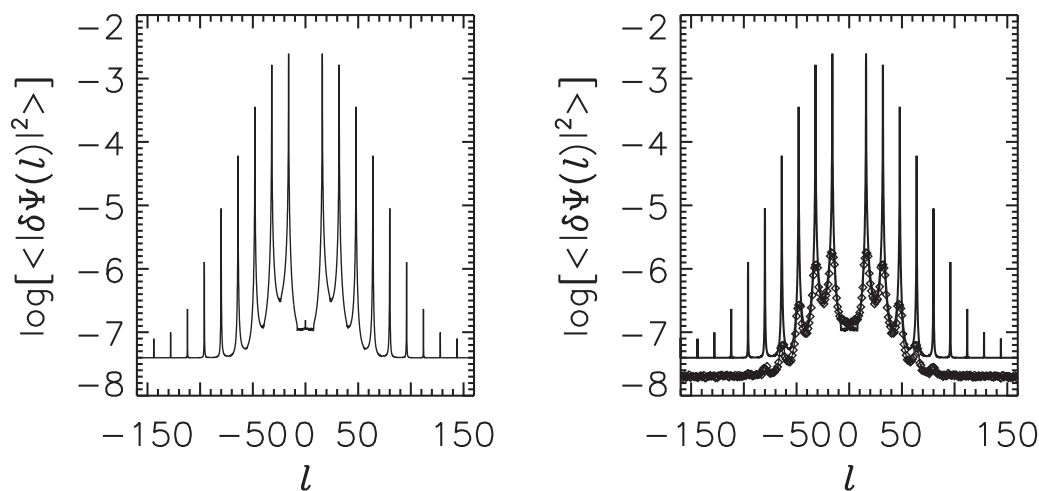


FIG. 4. Average square amplitude of the fluctuations in the frequency space. The left panel shows the results obtained analytically adding up the contributions of all modes given by (25). On the right, we compare the analytical calculations with numerical (symbols) simulations of the full model in Eq. (1).

differences need, however, to be discussed. First, a slight difference in the background for large frequencies can be attributed to accuracy of the calculations, as the amplitudes become very small and relative errors are large. The second difference is in the amplitudes of the frequencies very close to the peaks of the comb. In this case, the difference stems from the linear approximation. According to (25), the amplitude of the softmodes diverges when $q \rightarrow 0$ because $\Re(\lambda_{o,q}) \propto -q^2$. Then, these modes experience nonlinear saturation, and the results from the numerical simulation of the full model depart from the linear calculation.

The intensity fluctuations of the main frequency peaks will be dominated by other modes with $q = 0$. In particular, those with $\Re[\lambda_{1,0}] \sim -0.3$, which have a non-zero imaginary part, induce homogeneous oscillations of the pattern, precursors of a Hopf bifurcation for not so distant values of the parameters.²⁶ This mode excites equally positive and negative frequencies. Finally, the most damped mode, with $\Re[\lambda_{2M+1,0}] = -2$, corresponds to intensity fluctuations that affect positive and negative frequencies with an opposite sign, creating an unbalance in the symmetry of the frequency comb.²⁴ One can note that in the case of frequency combs created by cavity solitons, $L = 1$, and all modes of the cavity are excited. In this case, there are no soft modes, and only perturbations with $q = 0$ are possible.

V. CONCLUSION

In this article, we have investigated the fluctuation and correlation properties of Kerr optical frequency combs subjected to additive Gaussian white noise. We have provided a generic methodology to compute these estimators, and we have successfully compared our analytical results to numerical simulations.

Future work will be focused on exploring the fluctuation dynamics with different intracavity patterns,^{27,28} other nonlinearities,^{30–32} and extending the theory to a broader framework that would include quantum fluctuations.^{23,33–39}

ACKNOWLEDGMENTS

Y.K.C. acknowledges financial support from the University of Maryland through the Minta Martin Fellowship. P. Colet and D. Gomila acknowledge financial support from Agencia Estatal de Investigación (AEI, MCIU, Spain) and Fondo Europeo de Desarrollo Regional (FEDER, UE) under the Mariade Maeztu Program for units of Excellence in R&D (No. MDM-2017-0711).

DATA AVAILABILITY

The data that support the findings of this study are available from the corresponding author upon reasonable request.

REFERENCES

- 1 K. J. Vahala, "Optical microcavities," *Nature* **424**, 839–846 (2003).
- 2 A. Matsko *et al.*, "Review of applications of whispering-gallery mode resonators in photonics and nonlinear optics," *IPN Prog. Rep.* **42**, 1–51 (2005).
- 3 A. Chiasera *et al.*, "Spherical whispering-gallery-mode microresonators," *Laser Photon. Rev.* **4**, 457–482 (2010).
- 4 D. V. Strekalov *et al.*, "Nonlinear and quantum optics with whispering gallery resonators," *J. Opt.* **18**, 123002 (2016).
- 5 G. Lin, A. Coillet, and Y. K. Chembo, "Nonlinear photonics with high-Q whispering-gallery-mode resonators," *Adv. Opt. Phot.* **9**, 828–890 (2017).
- 6 T. J. Kippenberg, S. M. Spillane, and K. J. Vahala, "Kerr-nonlinearity optical parametric oscillation in an ultrahigh-Q toroid microcavity," *Phys. Rev. Lett.* **93**, 083904 (2004).
- 7 A. A. Savchenkov, A. B. Matsko, D. Strekalov, M. Mohageg, V. S. Ilchenko, and L. Maleki, "Low threshold optical oscillations in a whispering gallery mode CaF_2 resonator," *Phys. Rev. Lett.* **93**, 243905 (2004).
- 8 P. Del'Haye, A. Schliesser, O. Arcizet, T. Wilken, R. Holzwarth, and T. J. Kippenberg, "Optical frequency comb generation from a monolithic microresonator," *Nature* **450**, 1214–1217 (2007).
- 9 A. Pasquazi *et al.*, "Micro-combs: A novel generation of optical sources," *Phys. Rep.* **729**, 1–81 (2018).
- 10 J. Pfeifle *et al.*, "Optimally coherent Kerr combs generated with crystalline whispering gallery mode resonators for ultrahigh capacity fiber communications," *Phys. Rev. Lett.* **114**, 093902 (2015).

- ¹¹K. Saleh and Y. K. Chembo, "On the phase noise performance of microwave and millimeter-wave signals generated with versatile Kerr optical frequency combs," *Opt. Express* **24**, 25043–25056 (2016).
- ¹²L. A. Lugiato and R. Lefever, "Spatial dissipative structures in passive optical systems," *Phys. Rev. Lett.* **58**, 2209–2211 (1987).
- ¹³Y. K. Chembo, D. Gomila, M. Tlidi, and C. R. Menyuk, "Theory and applications of the Lugiato-Lefever equation," *Eur. Phys. J. D* **71**, 299 (2017).
- ¹⁴A. B. Matsko, A. A. Savchenkov, W. Liang, V. S. Ilchenko, D. Seidel, and L. Maleki, "Mode-locked Kerr frequency combs," *Opt. Lett.* **36**, 2845–2847 (2011).
- ¹⁵Y. K. Chembo and C. R. Menyuk, "Spatiotemporal Lugiato-Lefever formalism for Kerr-comb generation in whispering-gallery-mode resonators," *Phys. Rev. A* **87**, 053852 (2013).
- ¹⁶S. Coen, H. G. Randle, T. Sylvestre, and M. Erkintalo, "Modeling of octave-spanning Kerr frequency combs using a generalized mean-field Lugiato-Lefever model," *Opt. Lett.* **38**, 37–39 (2013).
- ¹⁷C. Godey, I. V. Balakireva, A. Coillet, and Y. K. Chembo, "Stability analysis of the spatiotemporal Lugiato-Lefever model for Kerr optical frequency combs in the anomalous and normal dispersion regimes," *Phys. Rev. A* **89**, 063814 (2014).
- ¹⁸P. Parra-Rivas, D. Gomila, M. A. Matias, S. Coen, and L. Gelens, "Dynamics of localized and patterned structures in the Lugiato-Lefever equation determine the stability and shape of optical frequency combs," *Phys. Rev. A* **89**, 043813 (2014).
- ¹⁹T. Miyaji, I. Ohnishi, and Y. Tsutsumi, "Bifurcation analysis to the Lugiato-Lefever equation in one space dimension," *Physica D* **239**, 2066–2083 (2010).
- ²⁰G. Kozyreff, "Localized Turing patterns in nonlinear optical cavities," *Physica D* **241**, 939–946 (2012).
- ²¹C. Godey, "A bifurcation analysis for the Lugiato-Lefever equation," *Eur. Phys. J. D* **71**, 131 (2017).
- ²²L. Delcey and M. Haragus, "Periodic waves of the Lugiato-Lefever equation at the onset of Turing instability," *Phil. Trans. R. Soc. Lond. A* **376**, 20170188 (2018).
- ²³Y. K. Chembo, "Quantum dynamics of Kerr optical frequency combs below and above threshold: Spontaneous four-wave mixing, entanglement, and squeezed states of light," *Phys. Rev. A* **93**, 033820 (2016).
- ²⁴D. Gomila and P. Colet, "Fluctuations and correlations in hexagonal optical patterns," *Phys. Rev. E* **66**, 046223 (2002).
- ²⁵G. Agez, M. G. Clerc, E. Louvergneaux, and R. G. Rojas, "Bifurcations of emerging patterns in the presence of additive noise," *Phys. Rev. E* **87**, 042919 (2013).
- ²⁶F. Leo, L. Gelens, P. Emplit, M. Haelterman, and S. Cohen, "Dynamics of one-dimensional Kerr cavity solitons," *Opt. Express* **21**, 9180–9191 (2013).
- ²⁷P. Parra-Rivas, D. Gomila, P. Colet, and L. Gelens, "Interaction of solitons and the formation of bound states in the generalized Lugiato-Lefever equation," *Eur. Phys. J. D* **71**, 198 (2017).
- ²⁸D. Walgraef, *Spatio-Temporal Pattern Formation* (Springer, New York, 1997).
- ²⁹C. W. Gardiner, *Handbook of Stochastic Methods* (Springer-Verlag, Berlin, 1983).
- ³⁰S. Diallo, G. Lin, and Y. K. Chembo, "Giant thermo-optical relaxation oscillations in mm-size whispering gallery mode disk-resonators," *Opt. Lett.* **40**, 3834–3837 (2015).
- ³¹G. Lin and Y. K. Chembo, "Phase-locking transition in Raman combs generated with whispering gallery mode resonators," *Opt. Lett.* **41**, 3718–3721 (2016).
- ³²G. Lin *et al.*, "Universal nonlinear scattering in ultra-high Q whispering gallery-mode resonators," *Opt. Express* **24**, 14880–14894 (2016).
- ³³L. A. Lugiato and F. Castelli, "Quantum noise reduction in a spatial dissipative structure," *Phys. Rev. Lett.* **68**, 3284–3286 (1992).
- ³⁴G. Grynberg and L. Lugiato, "Quantum properties of hexagonal patterns," *Opt. Commun.* **101**, 69–73 (1993).
- ³⁵A. Gatti, H. Wiedemann, L. A. Lugiato, I. Marzoli, G. L. Oppo, and S. M. Barnett, "Langevin treatment of quantum fluctuations and optical patterns in optical parametric oscillators below threshold," *Phys. Rev. A* **56**, 877–897 (1997).
- ³⁶R. Zambrini, M. Hoyuelos, A. Gatti, P. Colet, L. Lugiato, and M. San Miguel, "Quantum fluctuations in a continuous vectorial Kerr medium model," *Phys. Rev. A* **62**, 063801 (2000).
- ³⁷A. Gatti and S. Mancini, "Spatial correlations in hexagons generated via Kerr nonlinearity," *Phys. Rev. A* **65**, 013816 (2001).
- ³⁸I. Pérez-Arjona, E. Roldán, and G. J. de Valcárcel, "Theory of quantum fluctuations of optical dissipative structures and its application to the squeezing properties of bright cavity solitons," *Phys. Rev. A* **75**, 063802 (2007).
- ³⁹G.-L. Oppo and J. Jeffers, "Quantum fluctuations in cavity solitons," in *Quantum Imaging* (Springer, New York, 2007).